Update for E12-09-016: Measurement of the Neutron Electromagnetic Form Factor Ratio G_E^n/G_M^n at High Q^2

G. Cates, S. Riordan, and B. Wojtsekhowski
for the E12-09-016 Collaboration

January 5, 2010

1 Introduction

This document provides an update for E12-09-016, an experiment that will measure the ratio G_E^n/G_M^n up to $Q^2 = 10\,\mathrm{GeV}^2$. The original proposal and responses to the reviewer's questions of the proposal can be found at [1]. This experiment is one of three measurements of the ground-state electromagnetic nucleon form factors (FFs) that will be performed using the apparatus being constructed under the "Super-Bigbite" project. By emphasizing large-solid-angle detection and high luminosity, this experiment has a figure-of-merit that is 50 times higher than any competing effort to study G_E^n/G_M^n as of PAC34. Based on experience gained during E02-013 [2], we are confident that this experiment presents what is overwhelmingly the best opportunity to study G_E^n/G_M^n at high Q^2.

Nucleon form factors provide critical information on the structure of the nucleon. Their study has also taken on particular significance in recent years since the surprising discovery by Jones *et al.* that the ratio of the electric and magnetic form factors of the proton, G_E^p/G_M^p, decreases almost linearly with Q^2 [3]. The expectation had been that the quantity would be roughly constant. Indeed, this observation has forced a fundamental rethinking of nucleon structure, and caused considerable theoretical activity, as evidenced by nearly 500 citations. The various theoretical studies that have been performed in response to Ref. [3] represent some of the most sophisticated efforts to date to understand the nucleon in terms of QCD degrees of freedom, and have brought to light new features of nucleon structure that had not previously been appreciated.

The study of the electric form factor of the neutron, G_E^n, presents a tremendous opportunity. Not surprisingly, many of the theoretical efforts to understand the proton agree well with observations over the range of Q^2 that has been studied. The situation with the *neutron* is quite different. Presently, G_E^n is the least well known of the four nucleon FFs. Until quite recently, the highest Q^2 studied was $1.5\,\mathrm{GeV}^2$. Now, with the E02-013 results, measurements are available up to $3.4\,\mathrm{GeV}^2$. While of enormous interest, this range of Q^2 falls well below the range studied for the proton. Furthermore, the theories that explain well the proton data often disagree strongly with one another in their predictions for the neutron.

This experiment will provide precise measurements of G_E^n up to $Q^2 = 10\,\mathrm{GeV}^2$ using a technique that offers tremendous statistical power and that has now been proven to be highly successful. As will be discussed, we have made considerable progress over the past year in several areas. With the completion of the analysis of the three highest Q^2 points of E02-013, we have improved understanding of $^3\mathrm{He}$ as an effective neutron target. We have also made significant progress in our

development of the Super-Bigbite project which will provide much of the needed hardware. We are confident that this experiment can be ready to run as soon as beam is available following the 12 GeV upgrade.

2 Scientific Case

While the study of the nucleon form factors (FFs) has gained attention in recent years, our knowledge of G_E^n has lagged in terms of the range of Q^2 in which it has been measured. As will be discussed more below, measurements of G_E^n at high values of Q^2 provide a powerful means to distinguish between sophisticated models of the nucleon. Measurements of G_E^n are also necessary for performing flavor separations of the nucleon FFs, something of considerable value when comparing with *ab initio* Lattice QCD calculations. Measurements of G_E^n also provide critical constraints on the parameterization of generalized parton distributions (GPDs). As mentioned in the 2007 NSAC Long Range Plan, measurements of the ground-state form factors after the 12 GeV upgrade " ... remain the only source of information about quark distributions at small transverse distance scales."

An important development over the past year has been the completion of the analysis of E02-013, the final results of which are shown in Fig. 1. Shown with the red triangles, it can be seen that the E02-013 results fall very much in the midst some of the most successful theoretical efforts to understand the proton, and well above the historically often cited Galster parameterization. This, by itself, is quite interesting as it tends to support the emerging cleaner picture of the nucleon.

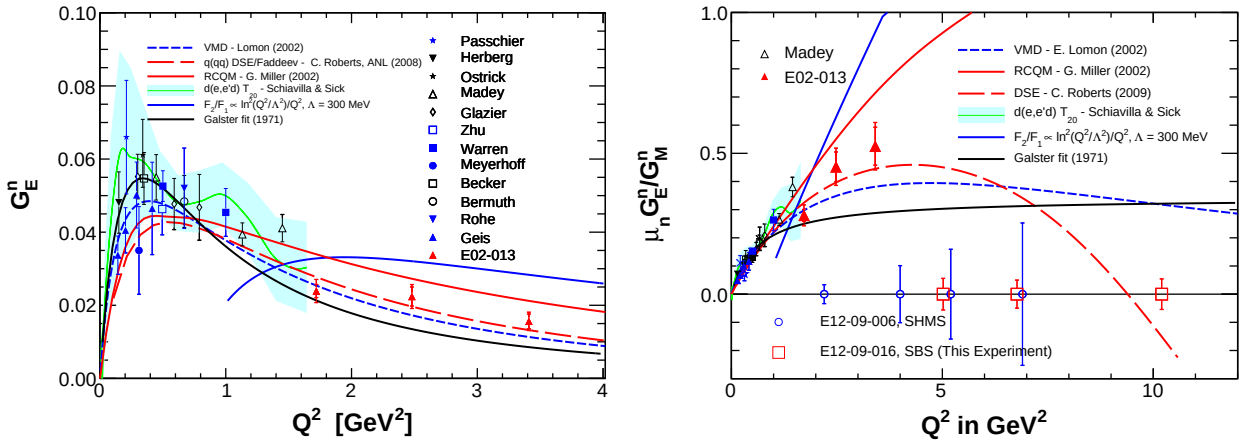

Figure 1: The final results for E02-013 and projected error bars for this experiment. A discussion of the curves can be found in the text.

Among the models that are quite consistent with the E02-013 data is a recent calculation from Argonne that utilizes QCD's Dyson-Schwinger equations (DSEs) [4]. The constituent quarks have their mass dynamically generated, and then serve as the degrees of freedom for a calculation using a Faddeev equation. While still a model, the DSE/Faddeev calculation contains elements, such as the dynamic generation of mass, that move in the direction of a true analytical solution. The model has relatively few parameters which are tuned to properties of the nucleon, such as its magnetic moments and masses. We note that the calculation incorporates di-quark degrees of freedom, and

has also been constructed such that it maintains essential symmetries of QCD such as Poincaré covariance and chiral symmetry.

Also shown, and again reasonably consistent with the data, is G. Miller's relativistic constituent quark light-front cloudy bag model (LFCBM), where a relativistic wavefunction of three massive quarks is constructed with the addition of a pion cloud [5]. This model uses light front dynamics which allows for a simple relation between the initial and final states of the wavefunction when scattering with a virtual photon. This model had particular success in describing the high Q^2 behavior of G_E^p.

An interesting feature of the DSE/Faddeev calculation and the LFCBM is that they both imply the dynamical importance of quark orbital angular momentum (OAM). Indeed, the importance of quark OAM has emerged in other experiments in recent years, including the observation of single-spin asymmetries at HERMES and COMPASS, and the behavior of the spin asymmetry A_1^n (measured in polarized deep inelastic scattering) at high values of Bjorken x. The discovery of Jones *et al.* [3] appears to have been pointing to important features of nucleon structure that had previously gone largely unrecognized.

A model that seems less consistent with our data is a modified pQCD calculation by Belitsky, Ji, and Yuan in which transverse momentum components were included in the quark wave functions [6]. This calculation was quite successful in reproducing the proton data, and like the above-mentioned models, it emphasized the importance of quark OAM. While it should be noted that Ref. [6] only explicitly addressed the proton, its apparent disagreement with the neutron is interesting.

Finally, we include in Fig. 1 a 2002 calculation due to E. Lomon [7], one example of several vector meson dominance (VMD) fits that have been published. Lomon's calculation contains interactions with five vector mesons and pQCD scaling described using $F_2/F_1 \sim 1/Q^2$. While less successful at high Q^2, Lomon's calculation is in good agreement at lower values of Q^2.

Of great importance to the discussion at hand, all four of the above-mentioned calculations diverge strongly from one another at high values of Q^2. In contrast, the above theories all reproduce the proton data reasonably well. Clearly, studies of the neutron can be of great value for discriminating between what are currently the most successful models of the nucleon. The importance of the nucleon FFs, however, is more far reaching than this. They are critical for constraining GPDs, for comparison with LQCD calculations, and for computing appropriate (relativistic) generalizations of charge and magnetic current distributions. The ground-state FFs represent fundamental properties of the nucleon that are critical to understanding nucleon structure.

3 Experimental Method Overview

Polarization observables have provided the most direct method to access the ratio of G_E/G_M for both the proton and neutron [8]. For our experiment we will measure a double polarization asymmetry in quasi-elastic scattering using the reaction $^3\overrightarrow{\mathrm{He}}(\vec{e}, e'n)pp$. As is described in some detail in our proposal, when scattering longitudinally polarized electrons from a polarized target, the polarization asymmetry is nearly proportional to G_E^n/G_M^n when the target spin is aligned perpendicular to the momentum transfer. The technique is much less sensitive to two photon-exchange effects compared to a Rosenbluth separation, with corrections estimated to be on the order $\alpha \sim 1/137$.

To study the quasi-elastic reaction $^3\overrightarrow{\mathrm{He}}(\vec{e}, e'n)pp$, the electron will be detected in coincidence with the recoiling nucleon. For the electron arm, we will use an upgraded version of the BigBite

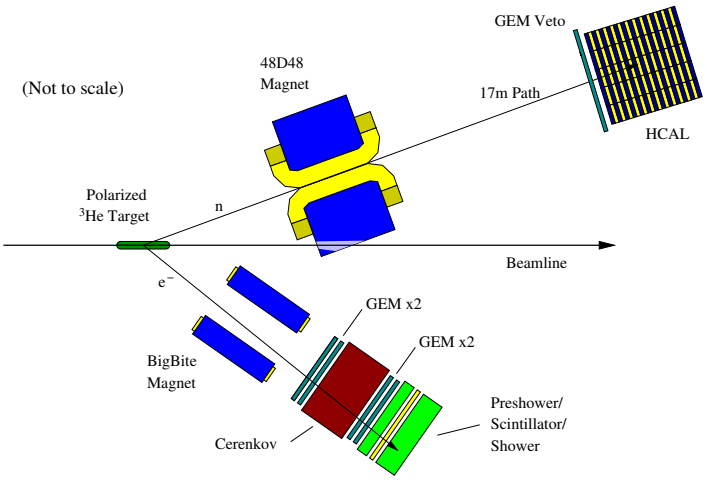

Figure 2: Proposed setup of E12-09-016 (not to scale).

spectrometer used during E02-013 that incorporates trackers based on GEM technology. For the neutron arm, we will use a hadron calorimeter, HCAL, that will also be used during GEp(5). The setup is shown schematically in Fig. 2. We note that this configuration differs very little from that shown in our original proposal, and details are presented in Section 4. The change saves both money and labor, and provides improved performance. As in the original proposal, the Brookhaven 48D48 magnet is placed between the target and HCAL to separate charged and uncharged particles as well as decrease the amount of accidental background from the target. Our proposed measurement points are found in Table 1.

An important consideration in our experiment is the degree to which inelastic events enter into the final data sample, a problem that is aggravated because of Fermi smearing. This issue becomes more pronounced at high Q^2 because the nucleon elastic cross section falls more rapidly than does the inelastic cross section in our range of W. During E02-013, however, we gained considerable experience dealing with this problem. By cutting hard on the missing transverse momentum of the recoil neutron, it is possible to discriminate strongly against inelastic events. The idea is as follows. In the absence of Fermi smearing, the momentum of the recoil neutron from an elastic-scattering event is completely determined by the kinematics of the detected electron. Even in the presence of Fermi smearing, however, the fraction of inelastic events is strongly suppressed as one demands near-elastic kinematics from the recoil neutron. Other cuts, such as the longitudinal momentum of the recoil neutron and missing mass are also of help.

While the above argument shows how it is possible to discriminate against inelastic events, the converse is also true. By demanding large transverse momentum from the recoil neutron, we can effectively select inelastic events. This will provide us with information on both the unpolarized cross section as well as the inelastic asymmetries. It is thus possible to formulate a Monte Carlo that is highly constrained by our own data. In fact, there is already significant data from unpolarized FF measurements that provides significant guidance. Also, to some extent, the inelastic cross sections are constrained by quark-hadron duality that ensures that behavior in the resonance region merges smoothly into the behavior observed in deep inelastic scattering. This is particularly true at our high values of Q^2 where resonance structure is strongly washed out. In the end, a full Monte Carlo

including detector acceptances and resolutions will be used to deconvolute the elastic and inelastic events as was done quite successfully in E02-013.

Q^2 (GeV^2)	E_i (GeV)	θ_e (deg)	p_e (GeV/c)	θ_n (deg)	p_n (GeV/c)
5.02	4.400	48.0	1.73	21.6	3.49
6.77	6.600	34.0	3.00	22.2	4.44
10.18	8.800	34.0	3.38	17.5	6.29

Table 1: A table of proposed measurement points.

It is worthwhile at this point to underscore the difference between the approach we are following here and an experiment such as E12-09-006, the Hall C experiment which plans to measure G_E^n up to $Q^2 = 7.0$ GeV^2. The Hall C experiment uses an alternative method to measure G_E^n/G_M^n measuring the polarization transfer to an unpolarized deuterium target. Statistically, such a method becomes difficult as one goes to higher Q^2 compared to our approach since the analyzing power of a polarimeter using a nuclear spin-orbit interaction drops roughly as $1/p$, where p is the momentum of the recoiling nucleon. Additionally, the physics of such a polarimeter requires measurements at small deflection angles, as the angle where the analyzing power maximizes for such a polarimeter also falls as $1/p$. This requirement puts a heavy demands going to larger acceptances as one must place detectors within the line of sight of the target. For the polarimetry method, the level of problems going to high Q^2 becomes apparent in the figure-of-merit. Using the previous Madey Hall C experiment as an example, going from $Q^2 = 1.5$ GeV^2 to 7 GeV^2, the naive figure-of-merit due to reduction in both the cross section and the analyzing power drops by a factor of 2500.

4 Technical Progress toward realizing the experiment

There have been several significant developments regarding this experiment in the last year. These involve the completion of the analysis of E02-013, a lower Q^2 version of this measurement, which demonstrates several techniques necessary for this analysis. Additionally, there has been progress regarding the realization of the Super-Bigbite spectrometer and the polarized ^{3}He target. We describe an update in the configuration of our neutron detection using the already proposed Super-Bigbite hadronic calorimeter, HCAL, which offers an alternative over the large wall of scintillator used in E02-013 (which was originally proposed for this experiment).

4.1 FSI calculations and effective neutron polarization in GEA framework

Since the neutron must be studied bound in a nuclear target, nuclear effects must be taken into account. These fall broadly into two categories: final state interactions (FSIs) and the effective polarization of the neutron. For the analysis of E02-013, these were calculated by M. Sargsian using the generalized eikonal approximation (GEA) [9]. The calculation utilized a ^{3}He wavefunction based on the Argonne V18 potential with a wavefunction calculated by the Bochum group. Also required to describe the photon coupling to the nucleon are nucleon form factor parameterizations, which were taken from a fit by J. Kelly [10] for G_E^p, G_M^p, and G_M^n. For G_E^n a range of values was studied centered on a Galster parameterization. The results were tested to ensure independence of the choice of assumed G_E^n value. Throughout the calculation, the acceptance of our spectrometer and the effects of our chosen kinematic cuts were taken into account.

The FSIs were due predominantly to rescattering from spectator nucleons and charge exchange effects. FSI's reduced the size of our measured asymmetry by just over 9.3, 7.7 and 3.7% for $Q^2 = 1.7,\ 2.5$, and $3.4\,\mathrm{GeV}^2$, respectively. What we found regarding the effective neutron polarization was quite interesting. The effective neutron polarization in experiments involving inclusive deep inelastic scattering have been shown by several calculations to be roughly 86%. In contrast, for our experiment, the effective polarizations are 96, 97, and essentially 100% for the three values of Q^2, respectively. The reason is quite interesting. Recall that we suppress inelastic events in our final data sample in large part by cutting on the transverse momentum of the recoil neutrons with respect to what they would have in the absence of Fermi smearing. This effectively selects out those portions of the ^{3}He wave function with lower momentum. In particular, it suppresses the degree to which the D state contributes, in which the three nucleons have their spins aligned opposite to the nuclear polarization.

While we have not yet done a full-blown GEA calculation for E12-09-016, the understanding and the machinery that has been developed for E02-013 are of tremendous value. We expect to examine these issues quite carefully as we prepare to run our experiment.

4.2 Evaluation of inelastic events in the neutral sample

Inelastic events enter into our sample due to Fermi smearing, detector resolution, and magnetically-shifted inelastic protons. Several steps are taken to ensure that these contributions are limited. First, we introduced more conservative cuts than were used for the E02-013 analysis. Second, by the addition of the 48D48 "BigBen" magnet a significant portion of inelastic events with charged protons are removed from our sample.

A Monte Carlo simulation was developed to evaluate the relative number of inelastic protons that would be deflected into our quasielastic cuts by the 48D48 magnet. We determined that these types of events comprised a relatively small fraction of the inelastic event sample, Fig. 3. On top of this, with the present status of the Super-Bigbite project, there will be additional GEM chambers constructed beyond what is needed for the electron arm. These will total an area of about 1.4×4.0 m^2, more than sufficient to cover the active area of HCAL. By placing these in front, they act as a veto, identifying protons very efficiently. By narrowing on the region around an HCAL hit, the misidentification of neutrons as protons due to accidental background will be less than 3%.

However, to ultimately deconvolute the contribution of these events from quasielastic neutral asymmetry, a Monte Carlo simulation must be performed. For such a calculation one in principle needs the inelastic cross section and asymmetry as well as the quasielastic cross section. For the E02-013 Monte Carlo, we used a simple on-shell moving nucleon initial state using a ^{3}He proton and neutron momentum distribution provided by R. Schiavilla. For E02-013's Q^2 range, the elastic cross section is primarily determined by G_M^n and a parameterization from J. Kelly [10] was used. For the inelastic contributions, since they are primarily single pion production events below $Q^2 = 5$ GeV^2, the MAID parameterization was used.

The final results of this calculation for E02-013 were successful in properly constraining these effects. For the $Q^2 = 3.4$ GeV^2 point, which was the only point where these effects were significant, we calculated a total of approximately 30,000 quasielastic neutral events and 6,000 inelastic. For this proposal at $Q^2 = 10$ GeV^2 we calculated we would have (after more conservative cuts and with the sweeper magnet) approximately 30,000 quasielastic events and 7,500 inelastic events. The final systematic uncertainty from the Monte carlo to the E02-013 point was less than 6%, and

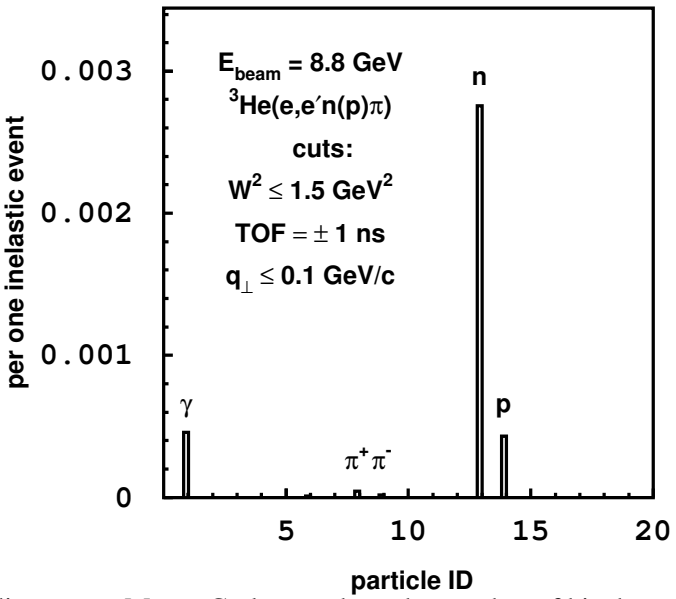

Figure 3: According to our Monte Carlo, we show the number of hits by particle type in HCAL for a single inelastic event for our $Q^2 = 10$ GeV^2 point.

a similar case should be present for this experiment. In the 12 GeV proposal we estimated a final 5% contribution, which has been demonstrated to be reasonable. Further work on this simulation will be performed to include off-shell nucleon effects.

Additionally, an effect which was not presented in the original proposal was the possible background production from nucleons passing through the perimeter of the BigBen magnet opening. A GEANT Monte Carlo simulation found that these "scraping events" contributed less than 0.1% to the final sample with all cuts.

4.3 Super-Bigbite Realization

In November 2008 the Super-Bigbite project was reviewed by a technical committee. The Conceptual Design Report (CDR) and the technical review reports can found at [11]. At PAC34 three new experiments that will use Super-Bigbite were approved: this experiment, neutron magnetic formfactor measurements (E12-09-019), and a SIDIS experiment (E12-09-018), the latter conditionally approved. This makes the collaboration behind the Super-Bigbite in Hall A much stronger. A funding proposal to DOE was submitted in November 2009 that will cover the whole experimental apparatus needed for three nucleon form factor experiments: E12-07-109 (referred to as GEp(5)), E12-09-016 (this experiment), and E12-09-019.

4.4 Hadronic Calorimeter

Several technical considerations make it preferable for us to use the proposed Super-Bigbite hadronic calorimeter, HCAL, over the BigHAND (the E02-013 neutron arm). This hadronic calorimeter is composed of 250 15×15 cm^2 modules consisting of interleaved layers of iron and scintillator. Along the edge of each of these modules are waveshifting bars which collect the light from the scintillator and transfer it to an attached photomultiplier tube. A more complete description can be found in the SBS CDR [11].

One significant practical advantage of the HCAL detector is that it is a part of the GEp(5) experiment, so the use of this detector will significantly reduce required manpower in preparation for this experiment. Such a calorimeter also offers several technical advantages over the existing neutron arm.

The threshold for such a detector can be set significantly higher than the neutron arm, dramatically reducing rates in individual counters for the neutron detector. By placing the threshold at an energy deposition of $50\ \mathrm{MeV}$ (compare to $3\ \mathrm{MeV}$) for our $Q^2 = 10\ \mathrm{GeV}^2$ running, we anticipate rates on the order of $50\ \mathrm{kHz}$ in the quasielastic cut region [12]. This is *orders of magnitude* less than the originally proposed neutron arm and effectively eliminates any deadtime effects. The detection efficiency of a hadronic calorimeter is greater than 95% for the proposed threshold of 25% of the average energy deposition. Due to the modular nature, the shape of this detector is much more flexible and can be matched directly to the BigBite acceptance. The means that using a "moon shape", we can achieve an identical useful solid angle at the same $17\ \mathrm{m}$ distance.

One technical point to be realized is an equivalent time-of-flight resolution as was the case for the neutron arm in E02-013, $\sigma_t \sim 300\ \mathrm{ps}$. Similar resolutions have been achieved for hadronic calorimeters in the past, e.g. the E864 calorimeter for AGS at Brookhaven [13]. We calculated that with the appropriate waveshifter configuration and readout we will be able to achieve at least the resolution as BigHAND in E02-013. Additionally, for our $Q^2 = 10\ \mathrm{GeV}^2$ we will also have an energy resolution from HCAL of about 30% which may aid in additional background discrimination, such as against photons.

4.5 Polarized $^3\mathrm{He}$ Target

For this experiment we utilize an upgraded version of the polarized ^{3}He target that has been constructed and successfully employed for a series of experiments in Hall A. This target is polarized using a hybrid alkali-metal spin exchange optical pumping technique, where an alkali-metal vapor, such as rubidium, is used to polarize a potassium vapor which then transfers its spin to the $^3\mathrm{He}$ nucleus.

To maintain a high polarization with the beam on the target, there are several significant changes to the target as was used in our previous G_E^n measurement. First, the utilization of spectrally narrow lasers which lead to a 60%+ polarization already implemented during last year's Hall A Transversity experiment. Second, the realization of convective has flow using a "double barrel transfer tube" design. This had been demonstrated at the time of the original proposal and a discussion can be found therein. Such flow has been studied in more detail since PAC34 and an accurate model that describes the gas velocity as a function of driving temperature has been developed. Additionally, progress has been made on the polarimetry techniques necessary for a convection cell using a "pulse NMR" system.

Finally, we plan to replace the glass target chamber with a metal chamber to withstand higher beam currents from 15 to $60\ \mu\mathrm{A}$. From such an addition, we also gain the flexibility to move the pumping chamber significantly farther from the target chamber, easing the technical space requirements in the target area. We plan to make the lower cell out of either aluminum or titanium, onto which we plan to place a gold coating. In the group of Ernst Otten, gold-coated glass was observed to have a relaxation time of 20 hours [14]. While this relaxation time is more than adequate, we note that there are reasons to believe that with the right preparation, a gold coating might well have a relaxation time significantly longer. Regardless, the results of reference [14] represent a proof-of-principle that gold coatings can be used for our purposes.

We have begun a series of tests to find the best way to apply gold coatings. In our first test, gold was evaporated onto the inner surface of glass under vacuum. The deposition was done for us by Zein-Eddine Meziani's group at Temple University. Unfortunately, this coating had a relaxation time of only a few hours. We are now trying a chemical deposition technique that was used by a group at Rutgers that were interested in obtaining a microscopically smooth surface. To monitor our progress, we are making measurements using an atomic force microscope that is available at the nanotechnology center across the street from the UVa physics building. This work will be part of the Ph.D. thesis by P. Dolph at the University of Virginia.

At present, we are studying what might be called the spin-exchange dynamics of convective-flow cells in parallel with developing coating technologies. From there we will begin building our first full-scale second-generation target cells. To make the cells resistant to depolarization from the beam, we plan to use a pumping volume that is fully twice that which was used during E02-013.

We believe we are being conservative in stating that we can have our first prototypes ready at least two years prior to the first beam being delivered to Hall A after the upgrade.

5 Beam Time Request

The beamtime request remains the same as in the original proposal. We introduce an updated set of errors that reflect our present understanding of the ^{3}He nucleus, Table 2. All other values from the proposal have remained the same. The total beam time request can be found in Table 3.

Q^2 (GeV^2)	time (hours)	Counts	G_E^n/G_M^n	stat. err.	sys. err.	G_E^n (Galster)	abs. err (G_M^n known)
5.02	38	20209	-0.1770	0.0271	0.0183	0.0046	0.0009
6.77	154	44928	-0.1918	0.0221	0.0209	0.0028	0.0004
10.18	864	29651	-0.2098	0.0323	0.0132	0.0014	0.0002

Table 2: Expected uncertainties for this proposal. The times given in this table are pure data taking times assuming 100% efficiency. They do not include the time needed for polarization measurements, optics data, or measurements of the dilution factor, $D_{\rm N}$. The number of counts is given for the cuts described in the original proposal [1].

	Beam Energy (GeV)	Data Taking Time (hours)	Total Time (hours)
Calibration Runs	4.400		48
$Q^2 = 5.0$ GeV^2	4.400	38	48
$Q^2 = 6.8$ GeV^2	6.600	154	192
$Q^2 = 10.2$ GeV^2	8.800	864	1080
Configuration Changes			16
Total		1055	1384

Table 3: Total beam time request for this experiment. A 100% beam efficiency and equipment availability has been assumed. Also, a 25% overhead on data taking time for target work and additional calibration measurements has been assumed.

References

[1] http://www.jlab.org/~riordan/gen2/

[2] Jeffereson Lab Hall A E02-013, G. Cates, N. Liyanage, and B. Wojtsekhowski,

[3] M.K. Jones *et al.*, Phys. Rev. Lett. **84**, 1398 (2000)

[4] C.D. Roberts *et al.*, Eur. Phys. J. **ST 140**, 53-116 (2007); I.C. Cloët *et al.*, Few-Body Systems **46**, 1-36 (2009).

032004 (2008).

[5] G. A. Miller and M. R. Frank, Phys. Rev. C **65**, 065205 (2002); G. A. Miller, Phys. Rev. C **66**, 032201 R (2002).

[6] A. V. Belitsky, X. Ji and F. Yuan, Phys. Rev. Lett. **91**, 092003 (2003).

[7] E. L. Lomon, Phys. Rev. C **64**, 035204 (2001).

[8] A.I. Akhieser, L.N. Rozenzweig and I.M. Shmushkevich, Sov. Phys. JETP **6**, 588 (1958); R.G. Arnold, C.E. Carlson, and F. Gross, Phys. Rev.C **23**, 363 (1981).

[9] M. M. Sargsian, arXiv:nucl-th/0110053 and private communication.

[10] J.J. Kelly, Phys. Rev. C 70 (2004) 068202

[11] The Super-Bigbite Spectrometer (SBS) Conceptual Design Report and SBS Technical review report can be found on the web-page
http://hallaweb.jlab.org/12GeV/SuperBigBite/SBS-CDR/

[12] http://www.jlab.org/~pavel/bw/hcal_a1000.pdf

[13] T.A. Armstrong *et al.*, Nuclear Instruments & Methods **A 406**, 227 (1998).

[14] A. Deninger, W. Heil, E.W. Otten, M. Wolf, R.K. Kremer and A. Simon, Eur. Phys. J. D **38**, 439 (2006).